# Measurements of Polarized-Neutron–Polarized-Proton Scattering: Implications for the Triton Binding Energy

W. S. Wilburn,[1] C. R. Gould,[2] D. G. Haase,[2] P. R. Huffman,[1] C. D. Keith,[2] J. E. Koster,[1,*] N. R. Roberson,[1] and W. Tornow[1]

[1] *Physics Department, Duke University, Durham, North Carolina 27708 and Triangle Universities Nuclear Laboratory, Durham, North Carolina 27708*

[2] *Physics Department, North Carolina State University, Raleigh, North Carolina 27695 and Triangle Universities Nuclear Laboratory, Durham, North Carolina 27708*

(Received 2 June 1993)

Measurements have been made of $\Delta\sigma_T$ for polarized neutrons incident on a polarized proton target from 3.65 to 11.60 MeV. In the energy range near 10 MeV, $\Delta\sigma_T$ is very sensitive to the nucleon-nucleon tensor interaction. Comparison of the data to potential-model predictions indicate that the tensor interaction is weak, resulting in values of the $^3S_1$-$^3D_1$ mixing parameter $\epsilon_1$ which are smaller than predicted by any nucleon-nucleon potential model. A smaller tensor force will bring the predictions of local potential models for the triton binding energy into closer agreement with the experimental value.

PACS numbers: 25.40.Dn, 13.75.Cs, 21.30.+y, 25.10.+s

A long-standing problem in nuclear physics has been the theoretical prediction of the triton binding energy [1]. All realistic and local nucleon-nucleon ($NN$) potentials predict too little binding. Many mechanisms have been proposed to increase the triton binding energy, among which are three-body forces and relativistic effects. Recent theoretical work, however, suggests that neither mechanism can contribute significantly [2,3]. In contrast, it is well established that the strength of the $NN$ tensor force below 50 MeV has a large influence on the triton binding energy [4]. $NN$ parameters above 50 MeV are not important for this problem as this is approximately the Fermi energy of the nucleons in the triton. Calculations [5] show that a weak tensor force at low energies will bring potential model predictions into closer agreement with the experimentally determined value.

In spite of its importance, both in the binding of few-nucleon systems and in the saturation of nuclear matter [5], the strength of the $NN$ tensor force is only loosely constrained by the existing data [6]. We have measured the spin-dependent difference in total cross section, $\Delta\sigma_T$, for the scattering of transversely polarized neutrons from transversely polarized protons below 12 MeV. These measurements cover a significant fraction of the energy range important to the triton binding energy. Our measurements indicate that the tensor force is indeed weak at low energies, possibly resolving the triton binding energy problem.

At low energies, the strength of the tensor interaction is parametrized by the isoscalar $^3S_1$-$^3D_1$ phase-shift mixing parameter $\epsilon_1$. $\Delta\sigma_T$ exhibits a large sensitivity to $\epsilon_1$ for neutron energies from 5 to 35 MeV [7]. In addition, $\Delta\sigma_T$ is insensitive to most other phase-shift parameters. The only significant sensitivity is to the $^1S_0$ and $^3S_1$ phase shifts which are constrained by experiment. In contrast, other observables sensitive to the tensor interaction such as the spin transfer parameter, $K_y^{y'}$, and the spin-correlation coefficient, $A_{yy}(\theta)$, are sensitive to the $P$ waves, which are much less well determined. Only in the special case $\theta = 90°$ is $A_{yy}$ independent of the $^1P_1$ phase shift.

$\Delta\sigma_T$ is measured using a polarized neutron beam incident upon a polarized proton target and is defined to be the total cross section with the spins antiparallel minus the total cross section with the spins parallel [8]:

$$\Delta\sigma_T = \sigma(\uparrow\downarrow) - \sigma(\uparrow\uparrow). \quad (1)$$

In both cases, the spins are transverse to the beam momentum. The present work consists of $\Delta\sigma_T$ measurements in the energy range 3.65 to 11.60 MeV. This energy range was chosen to include the zero crossing of $\Delta\sigma_T$ at approximately 5 MeV and the region of greatest sensitivity to $\epsilon_1$ around 10 MeV. Measurements made near the zero crossing are insensitive to most systematic effects.

The polarized proton target consists of titanium hydride, $TiH_2$, polarized by the brute-force method [9]. The target was prepared by pressing $TiH_2$ powder under a pressure of 1.5 GPa into a copper box, giving a proton target thickness of 0.2 atom/b. The target measures 14.0 × 34.1 mm, while the neutron beam at this point is 9.4 × 25.7 mm. The front and back of the box are open, so that no copper is exposed to the neutron beam. The polarization is obtained by cooling the target to a temperature of approximately 15 mK by a $^3$He-$^4$He dilution refrigerator in a 7 T magnetic field [10]. The field is produced by a superconducting split-coil solenoid. Target polarizations ranging from 40% to 50% have been obtained as measured by the neutron transmission asymmetry at 1.94 MeV.

The polarized neutron beam is produced as a secondary beam through a polarization-transfer reaction.



0031-9007/93/71(13)/1982(4)$06.00

For neutron energies below 6 MeV, the $^3$H$(\vec{p},\vec{n})^3$He reaction is used. Above 6 MeV the $^2$H$(\vec{d},\vec{n})^3$He reaction is used. In either case, the primary beam is produced by the TUNL atomic beam polarized ion source [11] and accelerated by a tandem Van de Graaff. The polarization of the primary beam is monitored by a carbon-foil analyzer and two silicon charged-particle detectors located at $\pm 40°$ lab angle. In the case of a proton beam the $^{12}$C$(\vec{p},p)^{12}$C reaction is used, while in the case of a deuteron beam the $^{12}$C$(\vec{d},p)^{13}$C reaction is used. In either case, the charged-particle polarimeter has been calibrated against a neutron polarimeter. The neutron beam is collimated by a combination of a copper precollimator and a polyethylene postcollimator. The neutrons are detected by liquid-scintillator cells placed at 0° and coupled to photomultiplier tubes.

$\Delta\sigma_T$ is determined by measuring the asymmetry in neutron transmission through the polarized proton target as the neutron spin is reversed. The asymmetry, $\varepsilon$, is given by

$$\varepsilon = \frac{N(\uparrow\uparrow) - N(\uparrow\downarrow)}{N(\uparrow\uparrow) + N(\uparrow\downarrow)}, \tag{2}$$

where $N(\uparrow\uparrow)$ and $N(\uparrow\downarrow)$ are the number of neutrons counted for the spins parallel and antiparallel. The asymmetry can be related to $\Delta\sigma_T$ by

$$\varepsilon = \tanh\left(\tfrac{1}{2}P_n P_T x \Delta\sigma_T\right), \tag{3}$$

$$\approx \tfrac{1}{2}P_n P_T x \Delta\sigma_T, \tag{4}$$

where $P_n$ is the neutron beam polarization, $P_T$ is the proton target polarization, and $x$ is the target thickness. The spin of the neutron beam is reversed at a rate of 10 Hz in an eight-step sequence ($\uparrow\downarrow\downarrow\uparrow\downarrow\uparrow\uparrow\downarrow$) designed to cancel systematic drifts to quadratic order in time [12]. This rapid reversal of spin allows an asymmetry to be calculated for each 800 ms spin sequence. Measurements must be made with the target unpolarized at each energy to determine the instrumental asymmetry.

The dilution refrigerator was started approximately 48 h prior to each set of measurements to allow the target temperature to stabilize. The first asymmetry measurement in each run was performed at 1.94 MeV to determine the product of target thickness and polarization, $xP_T$. At this energy, $\Delta\sigma_T$ is constrained by kinematics and the properties of the deuteron [13,14]. Calculations made from potential models, phase-shift analysis, and effective-range parameters agree to approximately $\pm 5\%$. Using these methods, we adopt a value of $938.9 \pm 39.1$ mb at 1.94 MeV [15]. Subsequent asymmetry measurements were made at the energies of interest. Finally, the target was warmed to approximately 1 K and the asymmetries measured at each energy with the target unpolarized.

The beam polarization was checked every few hours by inserting the carbon foil into the charged-particle polarimeter. When the $^3$H$(\vec{p},\vec{n})^3$He reaction is used as the neutron source, the neutron flux is proportional to the proton flux and was monitored by integrating the charge from the beam stop. For the $^2$H$(\vec{d},\vec{n})^3$He reaction, however, the neutron flux depends upon the tensor polarization of the deuteron beam. For this reason, the neutron flux was monitored by a small liquid organic scintillator placed between the neutron source and the polarized target. Proton beam currents were typically 1.0 $\mu$A, as determined by integrating the charge from the suppressed beam stop. The neutron polarization was typically 0.55 for spin up and $-0.45$ for spin down. Deuteron beam currents were kept below 0.5 $\mu$A to prevent heating of the polarized target. In this case we chose to change the neutron spin from polarized to unpolarized to avoid large changes in neutron flux due to deuteron tensor polarization [16]. The neutron polarization was typically 0.60.

The asymmetries for all spin sequences were averaged and normalized to the neutron beam polarization. Warm asymmetries are subtracted from cold asymmetries to remove instrumental effects. In the case of the zero-crossing measurements, two additional corrections have been applied. A multiplicative factor of typically 1.02 is applied at the lowest energies to correct for neutron depolarization in the target magnetic field and a multiplicative factor of typically 1.4 is applied to correct for the unpolarized neutron flux. These corrections have a negligible effect on the determination of the zero-crossing energy as they are simple scaling factors. The corrected asymmetry at each energy is normalized to the asymmetry at 1.94 MeV, which is a measure of the product of the target thickness and polarization, $xP_T$. This ratio is multiplied by the calculated value of $\Delta\sigma_T$ at 1.94 MeV to obtain $\Delta\sigma_T$ at the energy of interest.

The cross section differences, $\Delta\sigma_T$, measured in the present experiment are listed in Table I. The systematic uncertainties include uncertainties in the polarization-transfer coefficient for the neutron source reaction, in the analyzing power for the polarimeter, and in the value of $\Delta\sigma_T$ at the calibration energy. Figure 1 shows that the measured values of $\Delta\sigma_T$ are substantially higher than the prediction of the phase-shift analysis of Arndt, SP93 [17], indicating that the tensor force at low energies is much

TABLE I. Measured values of $\Delta\sigma_T$ with statistical and systematic uncertainties.

| $E_n$ (MeV) | $\Delta\sigma_T$ (mb) |
|---|---|
| 3.65 | $260.2 \pm 28.6 \pm 29.1$ |
| 4.42 | $45.9 \pm 35.3 \pm 4.8$ |
| 4.91 | $42.1 \pm 34.5 \pm 3.9$ |
| 5.21 | $-39.3 \pm 24.1 \pm 3.9$ |
| 5.81 | $-26.5 \pm 29.9 \pm 3.0$ |
| 6.25 | $-67.8 \pm 19.4 \pm 7.6$ |
| 7.43 | $-109.2 \pm 8.6 \pm 7.3$ |
| 9.57 | $-118.9 \pm 7.3 \pm 7.9$ |
| 11.60 | $-113.6 \pm 8.3 \pm 7.6$ |

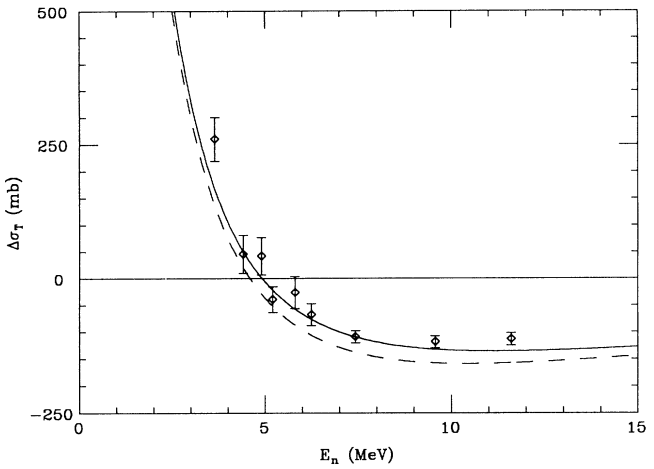


FIG. 1. Measured values of $\Delta\sigma_T$. The error bars represent the total uncertainty obtained by adding the statistical and systematic uncertainties in quadrature. The solid curve is the prediction of the Bonn B potential model, while the dashed curve is that of Arndt's phase-shift analysis SP93.

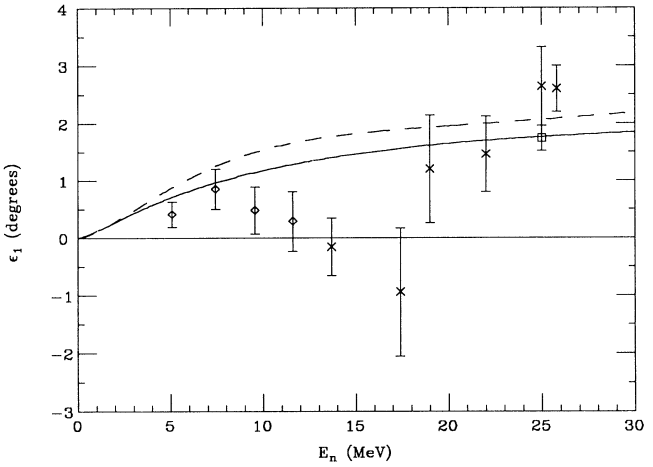


FIG. 2. Values of $\epsilon_1$ from analysis of the present data (diamonds) and from four previous measurements (crosses; see Table II for references). The solid curve is from the Bonn B potential model, while the dashed curve is from Arndt's phase-shift analysis SP93. Henneck's phase-shift analysis at 25 MeV is also shown (square).

weaker than the value obtained by fitting higher energy data that are relevant to $\epsilon_1$. In addition, the majority of our data are above the prediction of the Bonn B potential [5], a model which already assumes a weak tensor force.

To investigate this conclusion more quantitatively, we have performed a series of phase-shift analyses to determine the values of $\epsilon_1$. Here we report the results of the single-parameter phase-shift analysis. The results of the full phase-shift analyses are in agreement and will be presented in a longer paper. The data are fit by starting with the Bonn B potential-model phases and varying only $\epsilon_1$. Bonn B is chosen as it is the most realistic of the *np* potentials. In contrast, the Paris [18] and Nijmegen [19] potentials, for example, fit the $^1S_0$ phase shift only to *pp* scattering data. For the purpose of this analysis, the data in the range 3.65 to 6.25 MeV are fit to a smooth curve and the zero-crossing energy, $E_n = 5.08 \pm 0.10$ MeV, is determined [20]. The three measurements at the higher energies are treated separately. The results of the analysis are listed in Table II along with results obtained from four other measurements at energies from 13.7 to 25.8 MeV. In cases where a value of $\epsilon_1$ is not reported by the original authors, a single-parameter analysis such as the one described above is applied.

TABLE II. Values of the $\epsilon_1$ mixing parameter obtained by a single-parameter phase-shift analysis. All other phases are taken from the Bonn B potential model. $\epsilon_1$ values obtained from previous measurements in this energy range are listed. Except where indicated, a single-parameter phase-shift analysis has been applied to these data.

| $E_n$ (MeV) | $\epsilon_1$ (degrees) | Observable |
|---|---|---|
| 5.1 | $0.41 \pm 0.22$ [a] | $\Delta\sigma_T$ |
| 7.4 | $0.85 \pm 0.35$ [a] | $\Delta\sigma_T$ |
| 9.6 | $0.48 \pm 0.41$ [a] | $\Delta\sigma_T$ |
| 11.6 | $0.29 \pm 0.52$ [a] | $\Delta\sigma_T$ |
| 13.7 | $-0.16 \pm 0.50$ [b] | $A_{yy}(90°)$ |
| 17.4 | $-0.94 \pm 1.11$ [c] | $K_y^{y'}$ |
| 19.0 | $1.20 \pm 0.94$ [d] | $A_{yy}(90°)$ |
| 22.0 | $1.46 \pm 0.66$ [d] | $A_{yy}(90°)$ |
| 25.0 | $2.64 \pm 0.68$ [d] | $A_{yy}(90°)$ |
| 25.8 | $2.60 \pm 0.40$ [e] | $K_y^{y'}$ |

[a]Present data.
[b]Ref. [23]. Analysis performed by the original authors.
[c]Ref. [24].
[d]Ref. [25].
[e]Ref. [26]. Analysis performed by the original authors.

The $\epsilon_1$ values of Table II and the Bonn B and SP93 predictions for $\epsilon_1$ are plotted in Fig. 2. As can be seen, our results are quite consistent with those of previous measurements. The $\epsilon_1$ values are systematically smaller than the theoretical predictions below 20 MeV and clearly indicate that the tensor force is weaker even than that predicted by the Bonn B potential model. One might argue that this result is model dependent, but, as Table III shows, single-parameter phase-shift analyses using phases from Bonn B, Nijmegen [21], and SP93 all indicate a weak tensor force.

As can be seen from Fig. 2, Henneck's recent phase-shift analysis [22] at 25 MeV is also consistent with our values. His conclusion that the tensor force is strong below 160 MeV is therefore not applicable in our energy range. The apparent structure around 15 MeV has no known physical origin and is likely due to statistical fluc-

TABLE III. Comparison of the values of the $\epsilon_1$ mixing parameter obtained from the present data by single-parameter phase-shift analyses using the Bonn B potential model, the Nijmegen potential model, or Arndt's SP93 analysis, respectively.

| $E_n$ (MeV) | Bonn B | Nijmegen | SP93 |
|---|---|---|---|
| 5.1 | 0.41 | 0.45 | −0.11 |
| 7.4 | 0.85 | 1.00 | 0.39 |
| 9.6 | 0.48 | 0.65 | 0.02 |
| 11.6 | 0.29 | 0.31 | −0.32 |

tuations about a smoothly varying but small $\epsilon_1$. Nevertheless, more data are needed in the 10 to 20 MeV energy range to verify this conjecture. It should be pointed out that more conventional values for $\epsilon_1$ could be extracted from the data below 25 MeV if one were to allow the $^1S_0$ phase shift to deviate from its presently accepted values. However, the values would no longer vary smoothly with energy and would imply larger charge-independence breaking than presently accepted.

In summary, we have measured $\Delta\sigma_T$ for energies in the range from 3.65 to 11.60 MeV. In combination with data from four other experiments we have performed a single-parameter phase-shift analysis which yields consistently low values of the $\epsilon_1$ mixing parameter. These values indicate that the $NN$ tensor force is weaker than that predicted by potential models below 20 MeV. A weak tensor force at these energies will increase the calculated binding energy of the triton, bringing theoretical predictions into closer agreement with the experimentally determined value.

We wish to thank Dr. H. O. Klages at KFA Karlsruhe, Germany for providing the titanium hydride powder used in making the target. This research was supported in part by the U.S. Department of Energy, Office of High Energy and Nuclear Physics, under Grants No. DEFG05-91-ER40619 and No. DEFG05-88ER40441.

* Present address: Los Alamos National Laboratory, Los Alamos, NM 87545.

[1] B. F. Gibson, Nucl. Phys. **A543**, 1c (1992).
[2] A. Picklesimer, R. A. Rice, and R. Brandenburg, Phys. Rev. C **46**, 1178 (1992).
[3] F. Sammarruca, D. P. Xu, and R. Machleidt, Phys. Rev. C **46**, 1636 (1992).
[4] R. A. Brandenburg *et al.*, Phys. Rev. C **37**, 1245 (1988).
[5] R. Machleidt, Adv. Nucl. Phys. **19**, 189 (1989).
[6] G. S. Chulick *et al.*, Phys. Rev. C **37**, 1549 (1988).
[7] W. Tornow, in *Spin and Isospin in Nuclear Interactions*, edited by S. W. Wissink, C. D. Goodman, and G. E. Walker (Plenum Press, New York, 1991), p. 461.
[8] This choice of convention, antiparallel minus parallel, is the standard in $NN$ scattering.
[9] W. Heeringa, R. Aures, R. Maschuw, and F. K. Schmidt, Cryogenics **25**, 369 (1985).
[10] D. G. Haase, C. R. Gould, and L. W. Seagondollar, Nucl. Instrum. Methods Phys. Res., Sect. A **243**, 305 (1986).
[11] T. B. Clegg *et al.* (to be published).
[12] N. R. Roberson *et al.*, Nucl. Instrum. Methods Phys. Res., Sect. A **326**, 549 (1993).
[13] J. M. Blatt and L. C. Biedenharn, Phys. Rev. **86**, 399 (1952).
[14] R. Aures *et al.*, Nucl. Instrum. Methods Phys. Res., Sect. A **224**, 347 (1984).
[15] At $E_n = 1.94$ MeV we obtain from the full Bonn, Bonn A, Bonn B, Bonn C, SP93, and effective-range parameters the values of $\Delta\sigma_T$ = 899.8, 958.5, 959.2, 964.0, 879.2, and 878.9 mb, respectively.
[16] W. Heeringa, H. O. Klages, Chr. Wölfl, and R. W. Finlay, Phys. Rev. Lett. **63**, 2456 (1989).
[17] R. A. Arndt, phase-shift analysis SP93, 1993 (private communication).
[18] M. Lacombe *et al.*, Phys. Rev. C **21**, 861 (1980).
[19] M. M. Nagels, T. A. Rijken, and J. J. de Swart, Phys. Rev. D **17**, 768 (1978).
[20] W. S. Wilburn, Ph.D. thesis, Duke University, 1993.
[21] V. G. J. Stoks (private communication).
[22] R. Henneck, Phys. Rev. C **47**, 1859 (1993).
[23] M. Schöberl *et al.*, Nucl. Phys. **A489**, 284 (1988).
[24] M. Ockenfels *et al.*, Nucl. Phys. **A526**, 109 (1991).
[25] P. Doll *et al.*, in *Few Body XII*, edited by B. K. Jennings (TRIUMF, Vancouver, BC, Canada, 1989), p. C16.
[26] M. Ockenfels *et al.*, Nucl. Phys. **A534**, 248 (1991).